



PREPARED FOR  
AMERICAN SAMOA POWER AUTHORITY

A dark blue world map is visible in the background of the title section.

# WIND RESOURCE MAPS AND DATA OF AMERICAN SAMOA

OCTOBER 27, 2014

FINAL REPORT

---

TABLE OF CONTENTS

Introduction ..... 4

1. Project Scope..... 4

2. Wind Modeling..... 5

3. Wind Resource Measurements and Analysis..... 8

4. Map Validation and Adjustments..... 10

5. Time Series Meteorological Data and Climatological Variability ..... 12

6. Capacity Factor by Wind Turbine Classes..... 12

7. Summary ..... 15

Appendix ..... 16

**LIST OF FIGURES**

Figure 1. WRF grid configuration, with 27 km (red), 9 km (green) and 3 km (blue) domains. .... 7

Figure A 1. Mean annual wind speed at 30 meters. .... 17

Figure A 2. Mean annual wind speed at 50 meters. .... 18

Figure A 3. Mean annual wind speed at 200 meters. .... 19

**LIST OF TABLES**

Table 1. Mesoscale WRF model configuration ..... 6

Table 2. ASPA wind monitoring station summary ..... 8

Table 3. Observed and annualized mean wind speeds and heights for the 8 category A and B towers..... 9

Table 4. Comparison of observed and predicted mean speeds at 30 m height agl. Observed speeds have been adjusted to long-term conditions and extrapolated to 30 m height..... 11

Table 5. IEC Classification..... 13

Table 6. Composite Power Curve, Selected Turbine Models and IEC Class for American Samoa ..... 13

## INTRODUCTION

On behalf of the American Samoa Power Authority (ASPA), AWS Truepower (AWST) completed a comprehensive wind resource modeling and mapping study for the Island of Tutuila. The purpose of this project was to produce high-quality maps and gridded data sets characterizing the wind resource of American Samoa in support of renewable energy planning efforts.

Two major challenges to wind resource assessment in American Samoa are the islands' complex terrain and the limited availability of high-quality surface meteorological observations from weather stations. To overcome these challenges, AWS Truepower undertook a modeling study that incorporated state-of-the-art atmospheric models and leveraged data from ASPA's wind resource measurement program.

The wind resource was simulated over American Samoa at a horizontal grid resolution of 3 km using the Weather Research and Forecasting (WRF) Model, a leading open-source community model, and then further downscaled to 200 m resolution using AWS Truepower's WindMap code. WRF simulates the fundamental physics of the atmosphere, including the conservation of mass, momentum and energy and the moisture phases, using a variety of online, global, geophysical and meteorological databases. WindMap refines the WRF modeling by accounting for the localized effects of terrain and surface characteristics at a finer scale than can be resolved by WRF. In addition, data from 12 existing wind anemometer sites installed by the ASPA on the main island of Tutuila and one on neighboring Aunu'u were analyzed, and those data meeting quality standards were incorporated into the assessment.<sup>1</sup> This led to significant adjustments in the wind maps.

Gridded gross capacity factor (CF) estimates for different wind turbine classes were also developed. The capacity factor data provide a better perspective of wind development potential than conventional resource parameters such as mean wind speed or wind power density because it incorporates the productivity of suitable turbine models at every location. The CF data can be used by ASPA and project collaborators (including American Samoa agencies) in the development of potential wind estimates for the territory as a whole, or for administrative districts.

Last, AWST prepared hourly time series of wind and other meteorological data for each 3 km WRF grid cell over the project area. Areas representing the most energetic wind resource within each grid cell were identified, and data were developed to characterize the mean wind resource and resource variability at these locations. The data include annual and monthly average wind speeds for a typical meteorological year. The time series and accompanying statistics allow project planners and others to produce refined estimates of power production potential as well as to gauge extreme conditions that may affect turbine suitability. The datasets also allow planners to assess the variability of wind energy production over seasonal and annual time scales.

This report summarizes the modeling process, data review and validation, and adjustment of the wind maps and data sets.

### 1. PROJECT SCOPE

After the award of the contract, AWS Truepower worked with ASPA to define several important aspects of the project. The final scope of work completed by AWS Truepower incorporated several

---

<sup>1</sup> A separate report summarizes the existing meteorological stations on the Island of Tutuila, field visit findings and recommendations. AWS Truepower. 2014. Field Site Visit Report and Wind Resource Monitoring Recommendations.

---

enhancements and modified datasets better suiting the needs of ASPA. The final deliverables were as follows.

- Gridded wind and other meteorological data were produced for 6 heights above the surface (30, 50, 80, 100, 140, and 200 m) including:
  - Enhanced grid resolution of 200 m:
    - Surface type, land/water and percent of each
    - Average elevation above sea level
    - Surface roughness
  - Enhanced resolution of 1 km
    - Annual wind speed, wind power density, Weibull k, air density, temperature, wind rose, speed frequency distributions
  - Resolution of 3 km (original scope)
    - Monthly and diurnal wind speed, wind power density, Weibull k, temperature and air density
    - Monthly wind rose and speed frequency distributions
- Annual average gross capacity factor data were produced on a 200 m grid at the heights of 30, 50 and 80 m using a composite power curve based on wind turbine models that have been deployed in hurricane-prone areas for each IEC Class I, II and III
- Hourly time series of wind resource and climatological data were produced for a typical meteorological year (8760 hours) and for a full 15 years at heights 30, 50 and 80 m on a 3 km grid
  - Wind speed, direction, temperature, air density
- Climatological statistics were produced on a 3 km grid, including
  - Annual and monthly wind speed and standard deviation
  - Ratio of annual and monthly speeds to climatological average for each year
- Datasets were provided in GIS-compatible formats either as vector shape files or raster Geotiff files. Time series and statistics were provided in comma-separated text files.
- Additionally, an ArcReader project was prepared to allow users without GIS software to access and view the data.

## 2. WIND MODELING

AWS Truepower simulated the wind resource over American Samoa using WRF model version 3.5. WRF determines the evolution of atmospheric conditions within a region based on interactions among different elements in the atmosphere and between the atmosphere and the surface. Table 1 summarizes the WRF configuration used in this study. As indicated in this table, the simulations spanned the period January 1, 1999, to December 31, 2013, and the model output was stored every hour. The model initialization and boundary conditions were supplied by ERA-Interim (ERA-I), a historical global weather archive provided by the European Center for Medium Range Weather Forecasting.<sup>2</sup> The ERA-I data provide a snapshot of atmospheric conditions around the world at all levels of the atmosphere in

---

<sup>2</sup> ERA-Interim, which was developed by the European Centre for Medium-Range Weather Forecasts (ECMWF), utilizes a variety of observing systems which have been assimilated into a global three-dimensional grid by numerical atmospheric models at a spectral resolution of T255, or an approximate horizontal resolution of 79 km. See Dee, D. P., and Coauthors (2011). "The ERA-Interim reanalysis: configuration and performance of the data assimilation system". *Q.J.R. Meteorol. Soc.*, vol. 137, pp. 553–597.

intervals of six hours. High-resolution terrain, soil, and vegetation data were also used as input to the WRF simulations.

Table 1. Mesoscale WRF model configuration

Model	WRF v3.5.1
Grid configuration	27 km, 9 km, 3 km and One-Way Nesting with one-way nesting
Number of vertical levels	40
Time period	January 1, 1999 - December 31, 2013
Data storage interval	Hourly
Initialization data source	ERA-Interim
Sea-surface temperatures	ERA-Interim
High-resolution terrain	USGS GTOPO30 (30" resolution)
High-resolution land cover	Noah-modified 20-category IGBP MODIS (30" resolution)
Cumulus cloud scheme (27- and 9-km grids only)	Kain-Fritsch Eta
Planetary boundary layer scheme	2.5 Order Mellor-Yamada-Janjic (Janjic 2002) <sup>3</sup>
Spin-up period	24 hours before start of valid run
Assimilation Scheme Data assimilation scheme	Spectral nudging (von Storch et al. 2000) <sup>4</sup>
Length of run	1 month

The ERA-Interim data are on a relatively coarse grid (about 80-km spacing). To avoid generating noise at the boundaries of the simulation domain resulting from large jumps in grid cell size, it is recommended that mesoscale models such as WRF be run in nested grids of successively finer mesh size until the desired grid scale is reached. In this approach, each parent grid provides the initial fields and updated lateral boundary conditions for its immediate child grid, which then serves as the parent for the next grid, and so on. For this study, a nested grid arrangement with horizontal resolutions of 27 km – 9 km – 3 km, each with 40 vertical levels was used (Figure 1). The simulations capture the main factors influencing wind conditions on the islands, including synoptic weather patterns, island topographic influences, and land-sea breezes and other mesoscale circulations, at the 3 km resolution of the innermost WRF grid.

<sup>3</sup> Janjić Z (2002). "Nonsingular implementation of the Mellor–Yamada level 2.5 scheme in the NCEP meso model". NCEP Office Note No. 437, 60 pp.

<sup>4</sup> von Storch, H., H. Langenberg, and F. Feser, (2000). "A Spectral Nudging Technique for Dynamical Downscaling Purposes". *Mon. Wea. Rev.*, vol. 128, pp. 3664–3673.

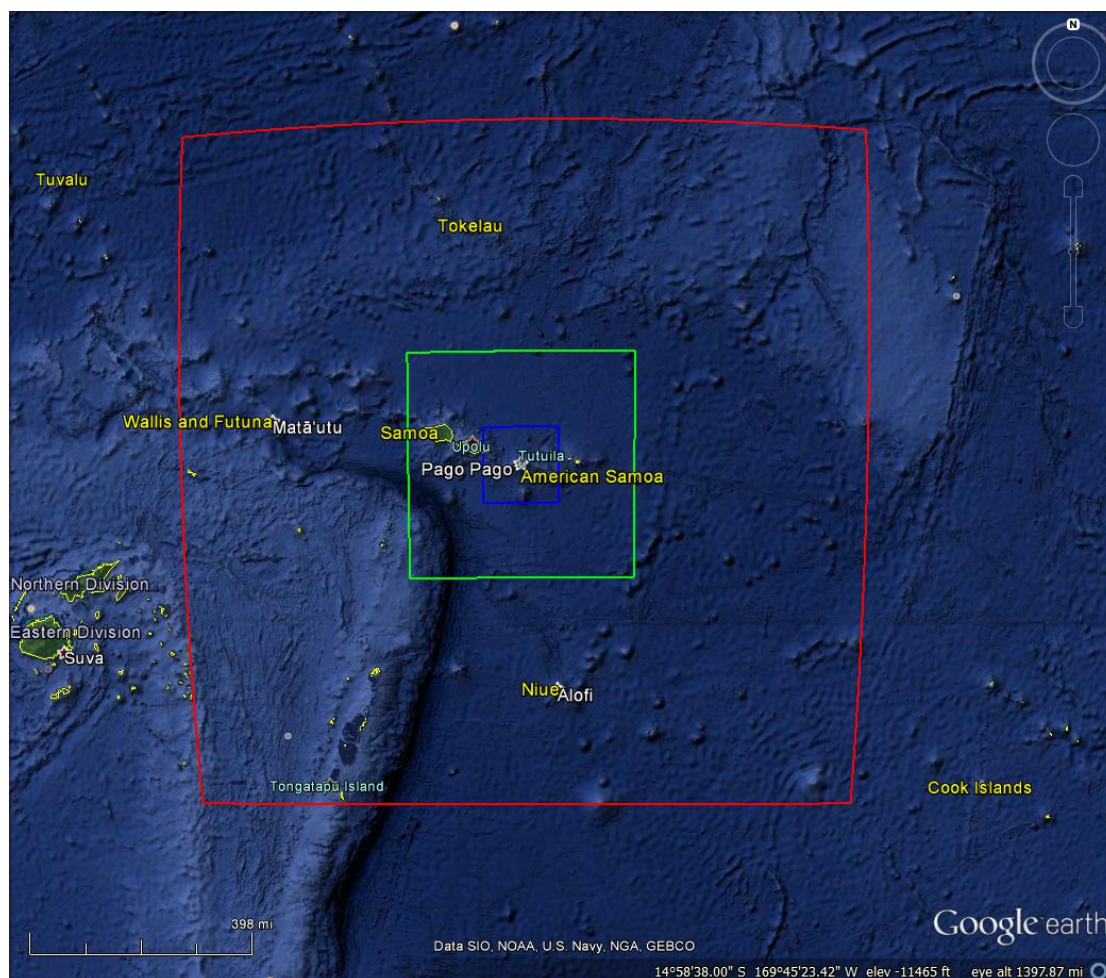


Figure 1. WRF grid configuration, with 27 km (red), 9 km (green) and 3 km (blue) domains.

Once the simulations were complete, a time series of meteorological variables including wind speed, direction, temperature, and pressure, was extracted for each 3 km WRF grid cell within 5 miles of land. The parameters provide all the information needed to characterize the wind resource and gross capacity factor.

In addition, the WRF output was summarized in wind statistics files, which were input into the WindMap software to downscale the 3 km simulations to a 200 m resolution. This process captures localized terrain and surface roughness influences that cannot be resolved at the WRF grid scale. The topographic data were from the 90 m resolution Shuttle Radar Topographic Mission (SRTM) dataset. The land use data were from the 300 m resolution Globcover 2009 dataset.<sup>5</sup> The land use was edited using aerial imagery to create a more accurate coastline and to account for changes that have occurred since the data were released.

<sup>5</sup> Université catholique de Louvain and European Space Agency (2011). "Globcover 2009: Products Description and Validation Report," 53 pp. See: [http://due.esrin.esa.int/globcover/LandCover2009/GLOBCOVER2009\\_Validation\\_Report\\_2.2.pdf](http://due.esrin.esa.int/globcover/LandCover2009/GLOBCOVER2009_Validation_Report_2.2.pdf)



### 3. WIND RESOURCE MEASUREMENTS AND ANALYSIS

#### Summary of Observations

The ASPA wind monitoring program consists of twelve monitoring stations installed between April and May 2012. Table 2 presents basic information about the masts including their geographic coordinates, elevations, periods of record, and sensor heights, along with our assessment of their overall quality and suitability for inclusion in this study (described below).

Table 2. ASPA wind monitoring station summary

Quality*	Mast	Site UTM Coordinates (WGS84, Zone 2S)		Elevation (m)	Period of Record	Monitoring Heights (m)		
		Easting	Northing			Wind Speed	Wind Direction	Temp
A	7797	525102	8416957	438	05/03/12 – 01/06/14	50.6, 35.1	32.5, 18.4	N/A
A	7798	523868	8412747	21	04/08/12 – 04/15/14	43.7, 34.5	37.6	N/A
A	7799	527984	8414432	39	04/10/12 – 08/01/13	44.8, 32.1	35.0	N/A
A	7803	524334	8418258	409	04/04/12 – 04/15/14	20.1, 14.4	18.4	N/A
B	7802	536327	8420229	46	04/07/12 – 09/27/13	24.7, 18.3	22.9	N/A
B	7805	542926	8421184	121	04/07/12 – 04/16/14	21.1, 17.3	20.6	N/A
B	7806	548180	8420689	44	04/09/12 – 04/17/14	24.5, 17.8	23.5	N/A
B	7808	541399	8423235	183	04/06/12 – 04/16/14	18.6, 12.9	15.8	N/A
C	7795	528303	8412706	20	04/04/12 – 07/05/13	20.2, 14.4	17.3	N/A
C	7804	526136	8412076	87	04/04/12 – 04/02/13	18.0, 12.2	15.2	N/A
C	7806	548180	8420689	44	04/09/12 – 04/17/14	24.5, 17.8	23.5	N/A
D	7800	533748	8422974	488	N/A	36.6, 32.0	34.1	N/A

\*A=Highest quality data, used in study; B=medium quality data, used in study; C=low quality, excluded from study; D=no data, excluded from study.

ASPA provided the data to AWS Truepower in a raw binary format; in addition, data for many of the stations were downloaded during the AWS Truepower site visits. Each data file contained 10-minute average wind speed and direction readings, along with their standard deviations; no temperature measurements were taken.

AWS Truepower inspected the data for completeness and reasonableness, and the towers were grouped into 4 quality classes, labeled A to D, as indicated in the table. The main issues addressed by the validation were equipment failures, periods of missing data, and tower blocking, or shadow. No data were provided for Mast 7800, and thus this mast was immediately excluded from the study. Following the data screening, the 11 remaining towers were further segmented by quality and completeness. Three towers, Masts 7795, 7804, and 7806, denoted class C in the table, were removed from the analysis due to instrument failures, inconsistent measurements, or problems with the data or documentation.

Of the eight remaining towers, we have the highest confidence in four (Masts 7797, 7798, 7799, and 7803), labeled class A. The other four (Masts 7802, 7805, 7806, and 7808), class B, exhibit inconsistencies when comparing different anemometer readings on each tower (for example, decreasing wind speed with increasing monitoring height). However, based on comparisons with other masts and reference data, we were able to choose a single sensor on each mast for analysis and comparison.



A summary of the observed and annualized mean speeds is provided in Table 3. The observed mean wind speed over each tower's period of record ranges from 3.93 m/s (at 43.7 m height) at Mast 7798 to 6.09 m/s (50.6 m height) at Mast 7797. These values may not be representative of year-round conditions, however. The annualized mean wind speed, which takes into account repeated months in the data record and weights each calendar month by its number of days, ranges from 3.92 m/s (43.7 m) at Mast 7798 to 6.24 m/s (50.6 m) at Mast 7797.

Table 3. Observed and annualized mean wind speeds and heights for the 8 category A and B towers.

Parameter	Mast 7797	Mast 7798	Mast 7799	Mast 7803
Measurement Height (m)	50.6	43.7	44.8	20.1
Mean Wind Speed (m/s)	6.09	3.93	4.03	5.45
Annualized Speed (m/s)	6.24	3.92	3.97	5.47
Annualized Wind Shear Exponent* (Heights)	0.293 (50.6 m / 35.1 m)	0.274 (43.7 m / 34.5 m)	0.219 (44.8 m / 32.1 m)	0.248 (20.1 m / 14.4 m)

Parameter	Mast 7802	Mast 7805	Mast 7806	Mast 7808
Measurement Height (m)	24.4	21.1	24.5	18.6
Mean Wind Speed (m/s)	5.25	5.17	4.07	4.17
Annualized Speed (m/s)	4.89	5.45	4.01	4.20
Annualized Wind Shear Exponent* (Heights)	N/A (Single Height)	N/A (Single Height)	N/A (Single Height)	N/A (Single Height)

\*Only Speeds > 4 m/s used in calculation

The wind shear, or rate of wind speed increase with height above ground, is defined by the exponent,  $p$  in the following power law:

$$U = U_0 (Z/Z_0)^p$$

where

$U$  = the unknown wind speed at height  $Z$  above ground;  
 $U_0$  = the known speed at a reference height  $Z_0$ ; and  
 $p$  = the shear exponent.

The observed shear exponent ranges from 0.219 (Mast 7799) to 0.293 (Mast 7797). It should be noted that these values could only be calculated for the first four masts, due to the availability of valid data for just one monitoring height at the remaining four. At each mast with two valid monitoring heights, the shear was calculated from the mean wind speeds at the highest and lowest monitoring levels based on concurrent valid records at both heights. Only wind speeds greater than 4 m/s, the range of interest for energy production, were used in the calculations. The wind shear at the other towers was estimated.

### Adjustment to Long-Term Conditions

Since the wind resource can vary significantly from year to year, it is important in wind resource assessment to adjust short-term wind measurements to long-term conditions. This was done for this project using a process called measure-correlate-predict (MCP), which relates short-term measurements at a target site to concurrent measurements at a long-term reference site. From this relationship, an estimate of the long-term mean wind speed at the target site can be obtained.

After evaluating a variety of data sources, the ERAI dataset was selected as the reference for this study. The MCP analysis was carried out in two steps. First, a linear regression was performed between observed daily mean wind speeds height for Mast 7803 and daily mean wind speeds from ERAI for the same location. Mast 7803 was chosen as the primary target mast for this analysis because it had the highest data recovery. The  $r^2$  correlation coefficient for this equation, 0.79, was deemed adequate for MCP. Substitution of the long-term ERAI mean into the equation yielded a long-term mean wind speed estimate of 5.46 m/s.

The long-term mean wind speeds at the other masts were then estimated using a similar technique, but with Mast 7803 now serving as the reference. The regression equations were established between each mast and Mast 7803 using concurrent hourly wind speeds; the  $r$ -squared values of these equations ranged from 0.65 (Mast 7808) to 0.88 (Mast 7802), and are deemed acceptable for this purpose. Substitution of the estimated long-term speed into the respective regression equations yields long-term mean wind speeds ranging from 3.94 m/s (44.8-m) at Mast 7799 to 5.99 m/s (50.6-m) at Mast 7797.

In the last step of the analysis, the long-term mean wind speeds at each mast were extrapolated to 30 m height using observed or estimated wind shear exponents. The results range from 3.58 m/s (Mast 7798) to 6.03 m/s (Mast 7803). A summary of the extrapolated wind speeds is provided in the following section.

## 4. MAP VALIDATION AND ADJUSTMENTS

Once the analysis of the wind resource measurements was completed, the long-term mean wind speeds at the class A and B stations were compared with the wind maps. The goal of this comparison was both to estimate the map accuracy and determine if any map adjustments were required.<sup>6</sup>

The comparison of the 200 m wind map with tower measurements was undertaken at 30 m height above ground. This height was chosen to limit the uncertainty due to wind shear. Despite the low height, it should be noted that considerable uncertainty remains in the estimated long-term mean wind speed at each tower.

As shown in Table 2, all of the tower data indicate the raw maps overestimate the wind resource to a considerable degree. The average bias is 1.2 m/s, or about 25% of the tower average. This bias is much larger than that generally observed in AWS Truepower mapping studies, an indication of the difficulty of modeling wind resources accurately in such complex terrain. Furthermore, the bias tends to be largest for towers at lower elevations. This suggests that a failure to fully resolve blocking by the island terrain (possibly due to the 3 km resolution of the WRF simulations) is largely responsible for the

---

<sup>6</sup> Other data sources besides the ASPA monitoring towers were evaluated, including NOAA stations; however, since the towers were short and the data records had significant gaps, these stations were not deemed suitable to be used in this study.

overestimation. A comparison of the map speeds with satellite-based QuikSCAT<sup>7</sup> wind speed estimates offshore tends to support this conclusion. Beyond the immediate influence of the islands, the QuikSCAT data show a moderate map bias of about 10-15% of mean speed.

Based on the results of these comparisons, it was decided to reduce the map wind speeds by a varying percentage ranging from about 10% at the highest elevations to 25% near sea level. This adjustment reduced the average bias at all eight ASPA towers to near zero and reduced the standard deviation of map errors slightly, from 0.52 m/s to 0.47 m/s. Offshore, the speeds were reduced in inverse proportion to distance from land, with no reduction beyond 0.5 miles.

The final adjusted annual mean wind speed maps at 30, 50, and 200 m are shown in the Appendix. In general, the wind speeds increase with increasing elevation, with lower speeds in the valleys where the flow is blocked by terrain. Higher wind speeds are also found farther offshore where the flow is less disturbed by the islands. Annual mean wind speed patterns are generally consistent at each height above ground level (agl), with mean speeds increasing with height.

Table 4. Comparison of observed and predicted mean speeds at 30 m height agl. Observed speeds have been adjusted to long-term conditions and extrapolated to 30 m height.

ID	Lat	Lon	Elev (m)	Obs Speed (m/s)	Raw Map (m/s)	Bias (m/s)	Adjusted Map (m/s)	Bias (m/s)
<b>7797</b>	-14.319	-170.767	438	5.14	6.53	1.39	5.62	0.48
<b>7798</b>	-14.357	-170.779	21	3.58	5.23	1.65	3.92	0.34
<b>7799</b>	-14.342	-170.740	39	3.60	5.06	1.46	3.85	0.24
<b>7803</b>	-14.307	-170.774	409	6.03	6.27	0.24	5.39	-0.64
<b>7802</b>	-14.290	-170.663	46	5.14	6.00	0.86	4.50	-0.64
<b>7805</b>	-14.281	-170.602	121	5.47	6.60	1.13	5.08	-0.39
<b>7806</b>	-14.285	-170.553	44	4.26	6.17	1.91	4.63	0.37
<b>7808</b>	-14.262	-170.616	183	4.67	5.60	0.94	4.48	-0.18
Avg				4.74	5.93	1.20	4.68	-0.05
SD						0.52		0.47

### Accuracy of the Wind Resource Maps

Our estimate of the overall uncertainty (one standard error) in the map speed estimates at any location is 10%. This is somewhat larger than usual for AWS Truepower maps for the reasons outlined above. With additional data, particularly using taller towers less subject to localized terrain and vegetation impacts, it is likely the uncertainty could be reduced. Recommendations for further wind monitoring have been provided to ASPA in a separate report.<sup>8</sup>

It should be stressed that the mean wind speed at any particular location may depart from the predicted value by even more than this uncertainty band, especially where the elevation, exposure, or surface

<sup>7</sup>JPL, SeaWinds on QuikSCAT Level 3 Daily, Gridded Ocean Wind Vectors Guide Document (version 1.1). Rapport technique, Jet Propulsion Laboratory, Pasadena, CA, USA. 2001. Available at <http://podaac.jpl.nasa.gov/quikscat/>.

<sup>8</sup> "Field Site Visit Report and Wind Resource Monitoring Recommendations", AWS Truepower Report, 29 August 2014.

roughness differs from that assumed by the model, or where the model scale is inadequate to resolve significant features of the terrain.

## 5. TIME SERIES METEOROLOGICAL DATA AND CLIMATOLOGICAL VARIABILITY

In addition to the wind maps, time series data sets were developed from the 15-year WRF runs for each 3 km grid point across the island and out to 5 miles offshore. The time series included wind speed and direction, temperature, pressure, and density at 30, 50 and 80-m above ground level.

The time series were then adjusted to reflect expected conditions at the best locations within each grid cell based on the assumption that these locations are the most likely to be developed for wind energy. This task was accomplished in several steps. First, the 200 m points within each 3 km grid cell with the top 20% of wind speed values at a height of 50 m agl were identified. The gridded model data were then interpolated and scaled to the predicted mean wind speeds for these locations. Temperature and pressure were adjusted to the mean elevation of the representative locations using standard lapse rates. The air density was calculated from the modeled temperature and pressure and corrected to the representative elevation.

Next, a typical meteorological year (TMY) consisting of 8760 hours was derived from the adjusted long-term time series for each grid cell. The TMY data were constructed from the long-term dataset by determining the cumulative probability distribution (CPD) of wind speeds for every month over the full period. The month with the lowest deviation from the long term CPD for that calendar month was selected. In this way, 12 representative month-long periods in the 15-year record were identified. The same months were used to construct the TMY at 30, 50 and 80 m heights above ground.

Land and ocean areas falling within a single WRF grid cell were treated separately. For grid cells that included both a land and water component, two representative time series were developed, one for onshore and one for offshore.

For each representative location identified for the TMY, summaries of the annual and monthly average wind speeds, the standard deviation of the wind speeds, and the ratios of the yearly and monthly speeds to the climatological average, were produced for each year. The data were summarized at 30, 50 and 80 m heights. The long-term hourly time series, TMY data set, and climatological statistics were provided in csv files for each WRF grid cell. The files are named by data type and grid cell location (e.g. 0001\_0001\_land\_ts.csv).

Annual mean wind speeds were fairly constant over the study period, with lower speeds in 1999, 2000, and 2011. Seasonal wind speed patterns are quite consistent over the island, with peak speeds between June and September or October. Diurnal mean wind vary less throughout the day. As expected, the diurnal patterns in wind speed differ less with height offshore than onshore, where the flow is disturbed by terrain and vegetation.

## 6. CAPACITY FACTOR BY WIND TURBINE CLASSES

Using the wind resource data generated in previous tasks, AWS Truepower developed gross capacity factor estimates for three hub heights and three turbine suitability classes. The method combines model-generated speed frequency distributions with a generic wind turbine power curve for each height and class combination, adjusted for air density, to determine the gross (without losses) output for each 200 m grid point across the island.

---

The recommended turbine class is determined by the expected mean wind speed, extreme wind speed, and turbulence intensity at 15 m/s. Table 4 shows the standard International Electrotechnical Commission (IEC)<sup>9</sup> classifications. IEC Class III turbines are generally designed to produce higher capacity factors at lower wind speeds than Class II and Class I turbines, but they are generally unsuitable for use at very windy sites. In contrast, Class I turbines are designed to tolerate stronger winds, but as a result typically produce less power relative to their rated capacity at low and moderate speeds. It should be noted that site climatic conditions, such as shear, air density, turbulence, and frequency distribution, can allow leeway in determining turbine suitability. It is ultimately up to the turbine manufacturer to determine whether a particular turbine model will be warranted for a particular site.

Table 5. IEC Classification

Wind Turbine Class		I	II	III	S
V <sub>ref</sub> (10 min)	m/s	50	42.5	37.5	Values are Specified by the designer
V <sub>e50</sub> (3 sec)	m/s	70	59.5	52.5	
V <sub>average</sub> (10 min)	m/s	10	8.5	7.5	
A	%	16			
B	%	14			
C	%	12			

After consulting with ASPA, AWS Truepower determined that the preferred hub heights for this analysis are 30, 50 and 80 m, and that the generic power curves should be based on composites of models that have previously been deployed and warranted on hurricane-prone islands like American Samoa. Based on this information, AWST created a series of composite power curves for representative IEC Class I, II and III turbine models at the requested hub heights, which were normalized to the turbine-specific rated capacity. Table 4 summarizes the turbine models used. It should be noted that these selections are based on current, commercially available turbine technology and do not consider future technology developments or the possible recertification of the turbines for higher IEC classes.

Table 6. Composite Power Curve, Selected Turbine Models and IEC Class for American Samoa

Model	Rotor Diameter (m)	Hub Height (m)	IEC	Rated Power	Composite (Height, IEC Class)
Vestas V80-2.0 MW	80	80, 95	IA	2	80, Class I
Vestas V100-2.0 MW	100	80, 95	IIB	2	80, Class II
Vestas V110-2.0 MW	110	80, 95	IIIA	2	80, Class III
Gamesa G90-2.0 MW	90	80, 100	IA	2	80, Class I
Gamesa G114-2.0 MW	114	80, 125, or site specific	IIA	2.5	80, Class II
Gamesa G114-2.5 MW	114	80, 125, or site specific	IIIA	2	80, Class III
SWT-3.0-108	108	site specific	IA	3	80, Class I
SWT-2.3-108	108	site specific	IIB	2.3	80, Class II
SWT-3.0-113	113	site specific	IIIA	3	80, Class III

<sup>9</sup> International Electrotechnical Commission – IEC Standard 61400-1 Wind Turbines Design Requirements – Ed. 3 2005.

Enercon E-44 / 900 kW	44	45, 55	IA	0.9	50, Class I
Vergnet GEV MP C	32	55/60	II, III	0.275	50, Class II/III
Gamesa G58-850 kW	58	44, 55	IIA, IIIB	0.85	50, Class II/III
Gamesa G52-850 kW	52	44, 55	IA	0.85	50, Class I
Vergnet GEV MP R	32	32	II, III, IV	0.275	30, All Classes
Norwin N29-225 kW	29	30, 40	Not Listed	0.225	30, All Classes

The following paragraphs provide some additional background on each turbine model. For further information, the manufacturers' published specifications should be consulted.

### Vestas

The Vestas V80-2.0MW turbine is the smallest currently offered by Vestas. The turbine has been installed in Aruba, Cuba, the Dominican Republic, New Caledonia, the Philippines, and Puerto Rico, all islands at risk of hurricanes. The turbine is available at hub heights from 60 m to 100 m, with the standard hub heights being 80 m and 95 m. The V100 and V110 models are suitable for Class II and Class III sites, respectively.

### Gamesa

The smallest turbine currently offered by Gamesa is the G52-850 kW. AWST considered the G52-850 kW and G58-850 kW turbine for the 50-m composite, based on the appropriate IEC class. These turbines are available at 45-m and 55-m hub heights. Gamesa has announced turbine sales in the Dominican Republic and has been in discussions with clients in other parts of the Caribbean region, which is considered to be impacted by hurricanes. The multi-MW Gamesa turbines are available at 80-m, 100-m and 125-m hub heights, or site specific hub heights.

### Siemens

The Siemens SWT-2.3-101 is the smallest turbine currently offered by Siemens. This turbine is offered at site specific hub heights; however, due to clearance restrictions the minimum hub height is likely to be 60 m or greater. Siemens has operating experience with the SWT-2.3-101 turbine in Puerto Rico, which is exposed to hurricanes. Siemens has two distinct turbine platforms for onshore application: the G2 platform, which is a geared turbine platform, and the D3 platform, which is a direct drive turbine platform. Direct drive turbines use a generator model that is designed to operate at slower revolutions; thus, they do not need a gearbox to increase the rotational speed. Both of these turbine options are available at hub heights of 80 m to 99.5 m or site specific. It should be noted that the IEC Class I and III turbines are part of the D3 platform, while the IEC Class II turbine is part of the G2 platform.

### Vergnet

The largest turbine available in the Vergnet line is the GEV HP 1 MW turbine, which has a hub height of 70 m. The smaller turbines, the GEV MP C and GEV MP R, are 275 kW with hub heights ranging from 30 m to 55 m. The Vergnet turbines are uniquely designed with a two-bladed rotor and are a guyed tower that can be lowered for severe weather conditions, such as a hurricane. Due to this technology, the turbines have been marketed in hurricane prone regions. Currently, Vergnet has 252 turbines in the Caribbean, including the Bahamas, Cuba, Puerto Rico, and the Virgin Islands, and 147 turbines in the South Pacific, including Chatham Island, New Caledonia, Vanuatu, Fiji, and the Cook Islands.

**Enercon**

Enercon has three small turbines available in the 800 kW to 900 kW range, with rotor diameters from 44 m to 53 m and hub heights from 45 m to 76 m. Enercon has one project in the Caribbean on Bonaire Island, using the E-44.

**Norwin**

Norwin has a single turbine model available with 30 m hub height. This turbine, the Norwin 29, is a stall-regulated turbine with a 29-m rotor diameter and can be either 200 kW or 225 kW. Currently, Norwin has one project in the Caribbean in the Dominican Republic.

**7. SUMMARY**

AWS Truepower has simulated the wind speed patterns over American Samoa using a 3-km mesoscale model run over the period 1999–2013 coupled with a microscale wind flow model run at 200 m resolution to better capture effects of localized terrain. Results were provided in various formats at several heights above the surface. Mean annual wind speed maps were generated by the model and adjusted to measurements from several towers installed by ASPA. The long term historical simulations and adjusted maps were used to characterize wind power density, Weibull  $k$ , wind rose, and speed frequency distributions. Long-term and TMY hourly time series were also provided at each 3-km location, as well as summary statistics at those same locations. Finally, gross capacity factor maps were provided using composite power curves developed from several commercially available turbines suitable for different IEC classes in hurricane-prone areas.



## APPENDIX



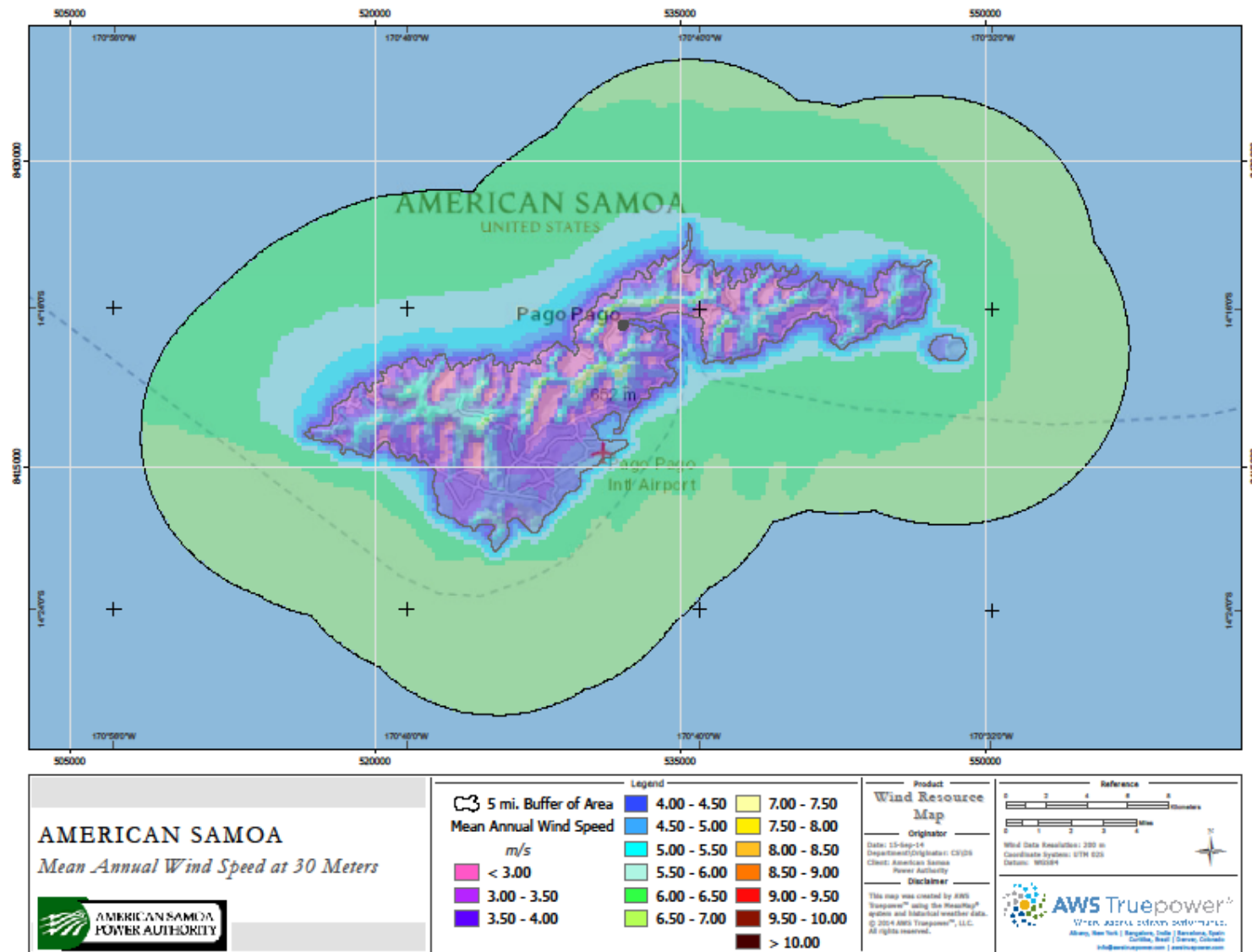


Figure A 1. Mean annual wind speed at 30 meters.

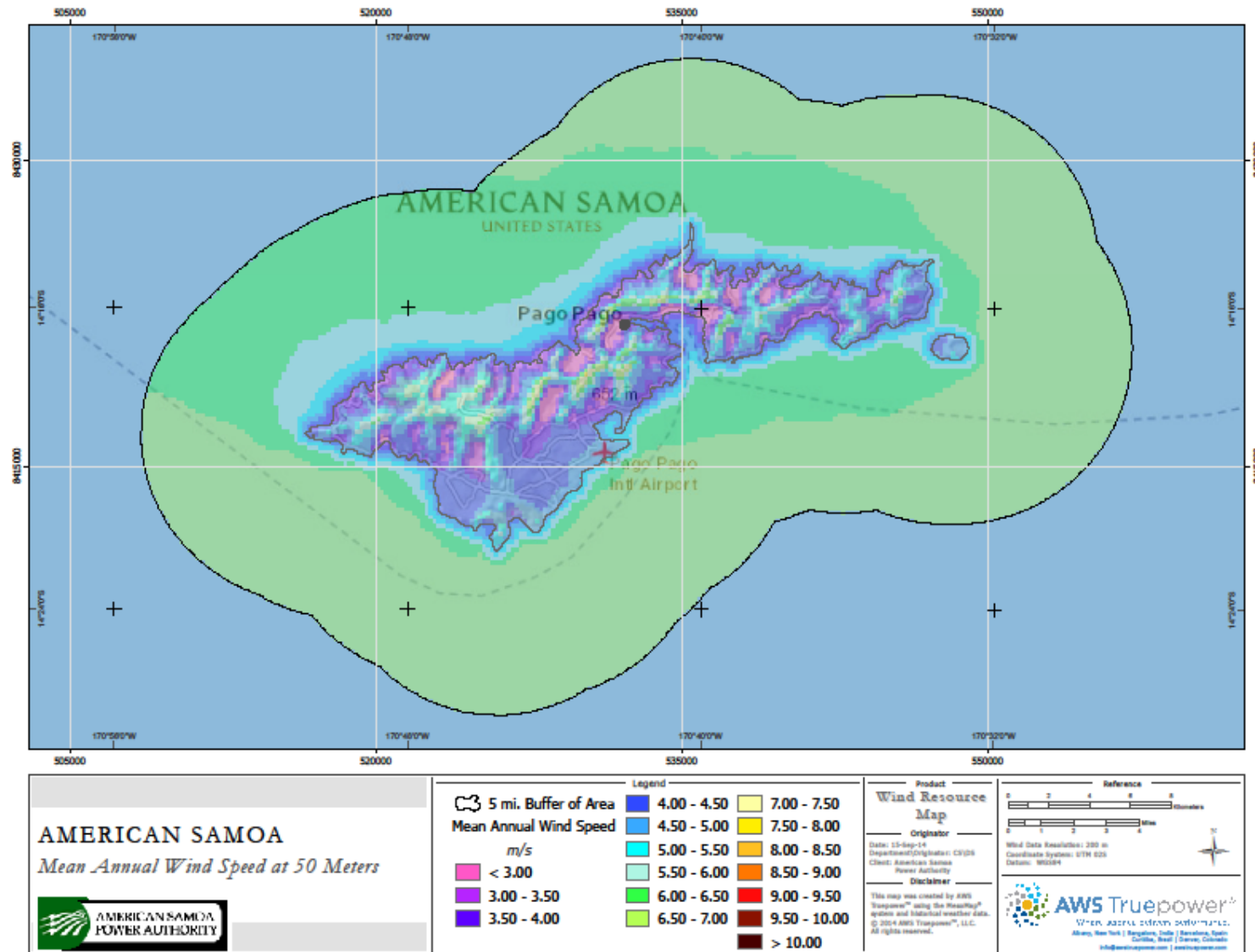


Figure A 2. Mean annual wind speed at 50 meters.

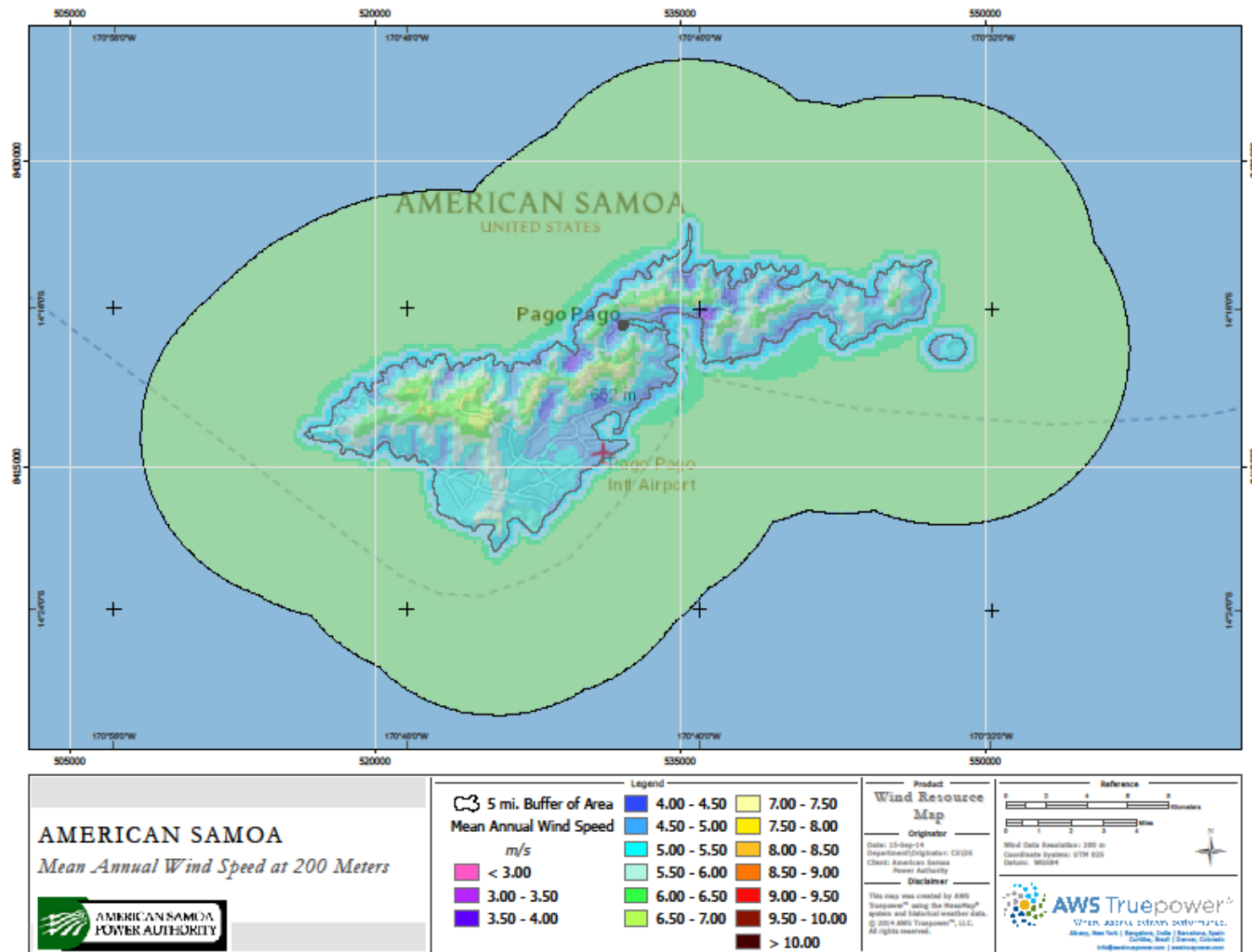


Figure A 3. Mean annual wind speed at 200 meters.